SUPPORTING INFORMATION

for

Supramolecular aggregation of Ni(salen) with $(C_6F_5)_2Hg$ and $[o\text{-}C_6F_4Hg]_3$

Mitsukimi Tsunoda, Martin Fleischmann, J. Stuart Jones, Nattamai Bhuvanesh, Manfred Scheer and François P. Gabbaï

This file includes:

Table S8. Selected derivative features of the electron density distribution function at BCPs cooresponding to intermolecular interactions involving mercury in [**B**-(Ni(salen))].

Figure S5. xyz plot of [**B**-(Ni(salen))], showing labeled BCPs cooresponding to intermolecular contacts not involving mercury.

Table S9. Selected features of the electron density distribution function at BCPs cooresponding to intermolecular contacts not involving mercury in [**B**-(Ni(salen))].

Table S10. Selected derivative features of the electron density distribution function at BCPs cooresponding to intermolecular contacts not involving mercury in [**B**-(Ni(salen))].

Figure S6. xyz plot of [**B**-(Ni(salen))], showing labeled BCPs cooresponding to selected intramolecular bonds in **B** and Ni(salen).

Table S11. Selected features of the electron density distribution function at selected intramolecular BCPs in [**B**-(Ni(salen))].

Table S12. Selected derivative features of the electron density distribution function at selected intramolecular BCPs in [**B**-(Ni(salen))].

Figure S7. xyz plot of [**B**-(Ni(salen))-THF-H_2O], showing labeled BCPs cooresponding to intermolecular interactions involving mercury.

Table S13. Selected features of the electron density distribution function at BCPs cooresponding to intermolecular interactions involving mercury in [**B**-(Ni(salen))-THF-H_2O].

Table S14. Selected derivative features of the electron density distribution function at BCPs cooresponding to intermolecular interactions involving mercury in [**B**-(Ni(salen))-THF-H_2O].

Figure S8. xyz plot of [**B**-(Ni(salen))-THF-H_2O], showing labeled BCPs cooresponding to intermolecular contacts not involving mercury between **B** and Ni(salen).

Table S15. Selected features of the electron density distribution function at BCPs cooresponding to intermolecular contacts not involving mercury between **B** and Ni(salen) in [**B**-(Ni(salen))-THF-H_2O].

Table S16. Selected derivative features of the electron density distribution function at BCPs cooresponding to intermolecular contacts not involving mercury between **B** and Ni(salen) in [**B**-(Ni(salen))-THF-H_2O].

Figure S9. xyz plot of [**B**-(Ni(salen))-THF-H_2O], showing labeled BCPs cooresponding to intermolecular contacts involving the H_2O and THF molecules.

Table S17. Selected features of the electron density distribution function at BCPs cooresponding to intermolecular contacts involving the H_2O and THF molecules in [**B**-(Ni(salen))-THF-H_2O].

Table S18. Selected derivative features of the electron density distribution function at BCPs cooresponding to intermolecular contacts involving the H_2O and THF molecules in [**B**-(Ni(salen))-THF-H_2O].

Figure S10. xyz plot of [**B**-(Ni(salen))-THF-H_2O], showing labeled BCPs cooresponding to selected intramolecular bonds in **B** and Ni(salen).

Table S19. Selected features of the electron density distribution function at selected intramolecular BCPs in [**B**-(Ni(salen))-THF-H_2O].

Table S20. Selected derivative features of the electron density distribution function at selected intramolecular BCPs in [**B**-(Ni(salen))-THF-H_2O].

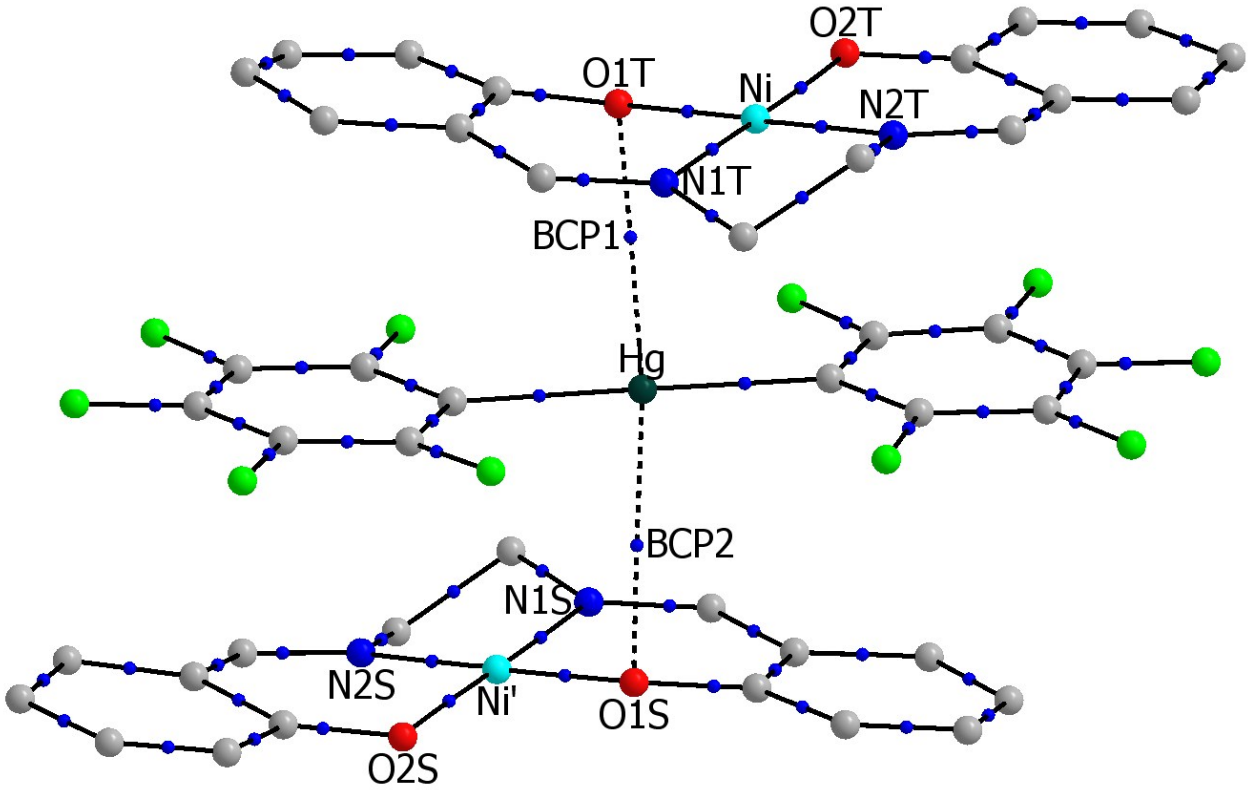

Figure S1. xyz plot of [**A**-(Ni(salen))], showing labeled BCPs cooresponding to intermolecular interactions involving mercury. BCPs are represented by blue spheres. Hydrogen atoms are omitted for clarity.

Table S1. Selected features of the electron density distribution function at BCPs cooresponding to intermolecular interactions involving mercury in [**A**-(Ni(salen))].

BCP No. (A-B)	$d_{A\text{-}BCP}$ (Å)	$d_{B\text{-}BCP}$ (Å)	ρ_{BCP} (e Å^{-3})	$\nabla^2\rho_{BCP}$ (e Å^{-5})	ε
1 (Hg-O1T)	1.666	1.451	0.09	0.93	0.17
2 (Hg-O1S)	1.698	1.483	0.08	0.83	0.13

Table S2. Selected derivative features of the electron density distribution function at BCPs cooresponding to intermolecular interactions involving mercury in [**A**-(Ni(salen))].

BCP No. (A-B)	H_{BCP} (Hartree Å^{-3})	G_{BCP} (Hartree Å^{-3})	δ(A,B)	$\oint_{A\cap B}\rho(r)$ (e Å^{-1})
1 (Hg-O1T)	0.003	0.06	0.09	0.48
2 (Hg-O1S)	0.003	0.06	0.08	0.31

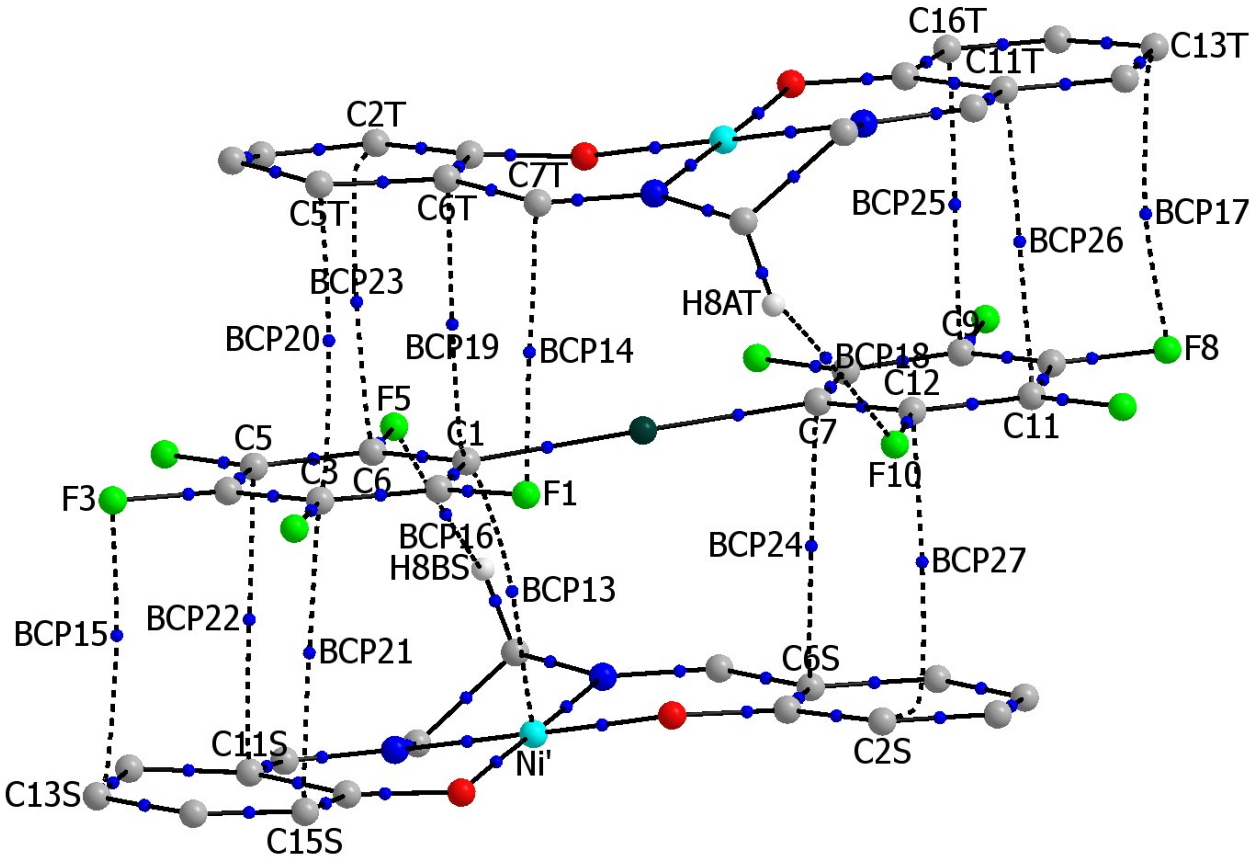

Figure S2. xyz plot of [**A**-(Ni(salen))], showing labeled BCPs cooresponding to intermolecular contacts not involving mercury. BCPs are represented by blue spheres. Selected hydrogen atoms are omitted for clarity.

Table S3. Selected features of the electron density distribution function at BCPs cooresponding to intermolecular contacts not involving mercury in [**A**-(Ni(salen))].

BCP No. (A-B)	$d_{A\text{-}BCP}$ (Å)	$d_{B\text{-}BCP}$ (Å)	ρ_{BCP} (e Å^{-3})	$\nabla^2\rho_{BCP}$ (e Å^{-5})	ε
13 (Ni'-C1)	1.764	1.776	0.04	0.36	4.11
14 (F1-C7T)	1.583	1.670	0.03	0.45	0.56
15 (F3-C13S)	1.545	1.798	0.03	0.48	0.92
16 (F5-H8BS)	1.571	1.207	0.02	0.45	0.09
17 (F8-C13T)	1.588	1.852	0.03	0.41	1.10
18 (F10-H8AT)	1.671	1.330	0.01	0.27	0.17
19 (C1-C6T)	1.745	1.726	0.04	0.41	8.96
20 (C3-C5T)	1.777	1.753	0.03	0.32	3.37
21 (C3-C15S)	1.715	1.764	0.03	0.33	0.23
22 (C5-C11S)	1.698	1.726	0.04	0.40	1.09
23 (C6-C2T)	1.683	1.779	0.04	0.37	2.76
24 (C7-C6S)	1.699	1.727	0.04	0.43	2.52

25 (C9-C15T)	1.669	1.728	0.04	0.39	0.51
26 (C11-C11T)	1.717	1.737	0.04	0.39	1.44
27 (C12-C2S)	1.684	1.829	0.03	0.36	3.59

Table S4. Selected derivative features of the electron density distribution function at BCPs cooresponding to intermolecular contacts not involving mercury in [**A**-(Ni(salen))].

BCP No. (A-B)	H_{BCP} (Hartree Å^{-3})	G_{BCP} (Hartree Å^{-3})	δ(A,B)	$\oint_{A\cap B}\rho(r)$ (e Å^{-1}) [a]
13 (Ni'-C1)	0.005	0.02	0.02	N/A
14 (F1-C7T)	0.008	0.02	0.01	0.06
15 (F3-C13S)	0.007	0.03	0.02	0.08
16 (F5-H8BS)	0.009	0.02	0.01	0.05
17 (F8-C13T)	0.006	0.02	0.01	0.05
18 (F10-H8AT)	0.006	0.01	0.01	0.03
19 (C1-C6T)	0.005	0.02	0.01	N/A
20 (C3-C5T)	0.004	0.02	0.01	N/A
21 (C3-C15S)	0.000	0.02	0.01	N/A
22 (C5-C11S)	0.005	0.02	0.02	N/A
23 (C6-C2T)	0.005	0.02	0.01	N/A
24 (C7-C6S)	0.005	0.02	0.02	N/A
25 (C9-C15T)	0.005	0.02	0.02	0.17
26 (C11-C11T)	0.005	0.02	0.02	0.20
27 (C12-C2S)	0.005	0.02	001	N/A

a) Some values of $\oint_{A\cap B}\rho(r)$ (e Å^{-1}) could not be determined, due to integration of some atoms with the 'Promega' algorithm instead of the 'Proaim' algorithm within the AIMAll program.

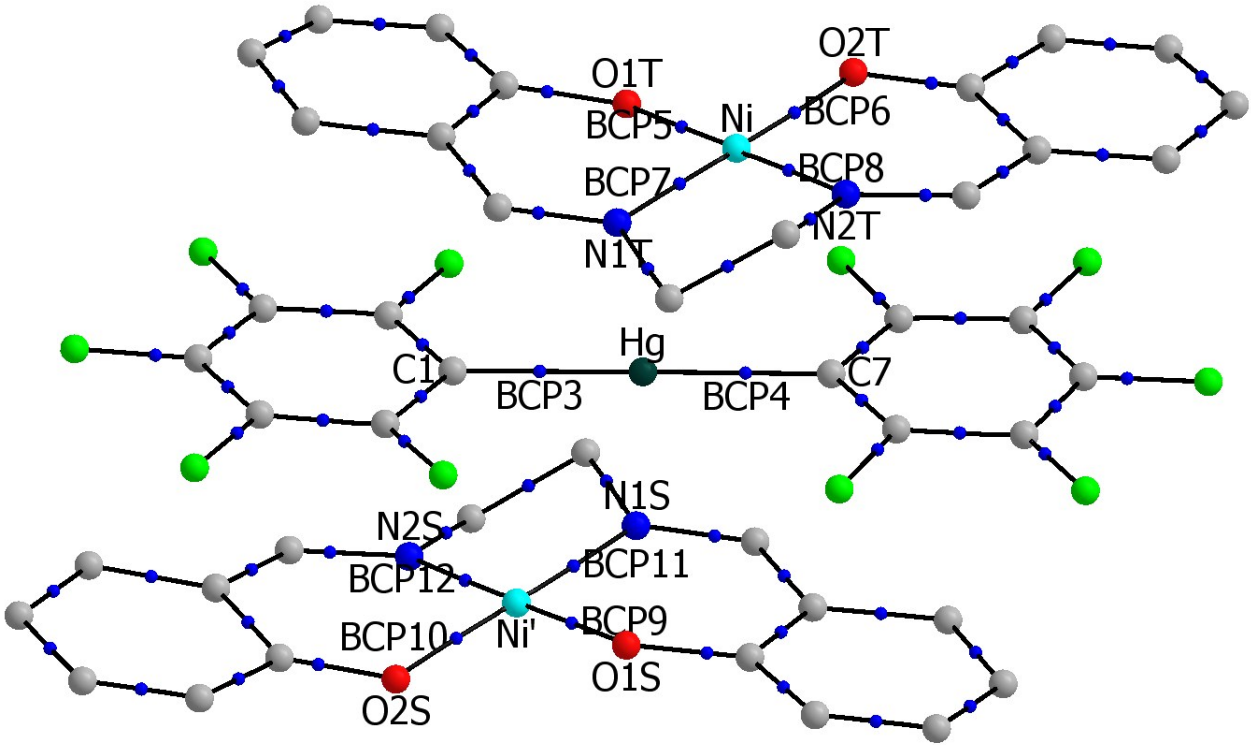

Figure S3. xyz plot of [**A**-(Ni(salen))], showing labeled BCPs cooresponding to selected intramolecular bonds in **A** and Ni(salen). BCPs are represented by blue spheres. Hydrogen atoms are omitted for clarity.

Table S5. Selected features of the electron density distribution function at selected intramolecular BCPs in [**A**-(Ni(salen))].

BCP No. (A-B)	$d_{A\text{-}BCP}$ (Å)	$d_{B\text{-}BCP}$ (Å)	ρ_{BCP} (e Å^{-3})	$\nabla^2\rho_{BCP}$ (e Å^{-5})	ε
3 (Hg-C1)	1.127	0.950	0.87	3.40	0.03
4 (Hg-C7)	1.120	0.937	0.91	3.53	0.03
5 (Ni-O1T)	0.884	0.942	0.73	16.85	0.10
6 (Ni-O2T)	0.894	0.958	0.72	15.93	0.10
7 (Ni-N1T)	0.897	0.980	0.80	13.00	0.04
8 (Ni-N2T)	0.887	0.961	0.85	13.97	0.04
9 (Ni'-O1S)	0.881	0.938	0.78	17.29	0.10
10 (Ni'-O2S)	0.891	0.954	0.73	16.29	0.11
11 (Ni'-N1S)	0.899	0.982	0.79	12.92	0.04
12 (Ni'-N2S)	0.888	0.963	0.85	13.85	0.04

Table S6. Selected derivative features of the electron density distribution function at selected intramolecular BCPs in [**A**-(Ni(salen))].

BCP No. (A-B)	H_{BCP} (Hartree Å^{-3})	G_{BCP} (Hartree Å^{-3})	δ(A,B)	$\oint_{A\cap B}\rho(r)$ (e Å^{-1})[a]
3 (Hg-C1)	-0.409	0.65	0.84	1.75
4 (Hg-C7)	-0.436	0.68	0.85	1.93
5 (Ni-O1T)	-0.086	1.27	0.64	1.76
6 (Ni-O2T)	-0.056	1.17	0.60	1.48
7 (Ni-N1T)	-0.187	1.10	0.69	1.50
8 (Ni-N2T)	-0.227	1.21	0.71	1.56
9 (Ni'-O1S)	-0.090	1.30	0.64	1.58
10 (Ni'-O2S)	-0.061	1.20	0.60	N/A
11 (Ni'-N1S)	-0.180	1.08	0.68	1.50
12 (Ni'-N2S)	-0.180	1.08	0.68	1.50

a) Some values of $\oint_{A\cap B}\rho(r)$ (e Å^{-1}) could not be determined, due to integration of some atoms with the 'Promega' algorithm instead of the 'Proaim' algorithm within the AIMAll program.

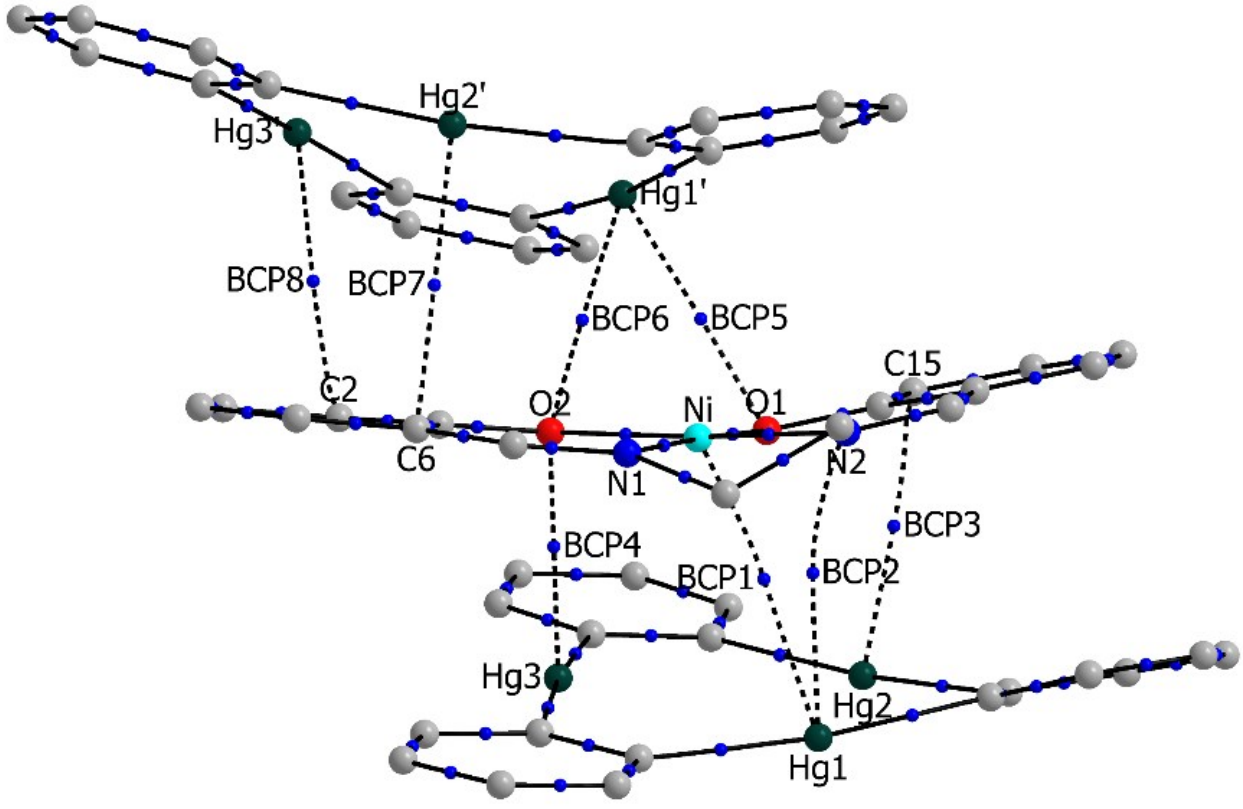

Figure S4. xyz plot of [**B**-(Ni(salen))], showing labeled BCPs cooresponding to intermolecular interactions involving mercury. BCPs are represented by blue spheres. Fluorine and hydrogen atoms are omitted for clarity.

Table S7. Selected features of the electron density distribution function at BCPs cooresponding to intermolecular interactions involving mercury in [**B**-(Ni(salen))].

BCP No. (A-B)	$d_{A\text{-}BCP}$ (Å)	$d_{B\text{-}BCP}$ (Å)	ρ_{BCP} (e Å^{-3})	$\nabla^2\rho_{BCP}$ (e Å^{-5})	ε
1 (Hg1-Ni)	1.834	1.711	0.06	0.54	1.71
2 (Hg1-N2)	1.828	1.668	0.06	0.53	3.83
3 (Hg2-C15)	1.677	1.484	0.09	0.93	0.35
4 (Hg3-O2)	1.576	1.362	0.12	1.34	0.13
5 (Hg1'-O1)	1.651	1.440	0.09	0.99	0.24
6 (Hg1'-O2)	1.636	1.423	0.09	1.05	0.17
7 (Hg2'-C6)	1.773	1.605	0.07	0.63	0.58
8 (Hg3'-C2)	1.804	1.607	0.06	0.56	0.53

Table S8. Selected derivative features of the electron density distribution function at BCPs cooresponding to intermolecular interactions involving mercury in [**B**-(Ni(salen))].

BCP No. (A-B)	H_{BCP} (Hartree Å^{-3})	G_{BCP} (Hartree Å^{-3})	δ(A,B)	$\oint_{A\cap B}\rho(r)$ (e Å^{-1})
1 (Hg1-Ni)	0.006	0.03	0.05	0.17
2 (Hg1-N2)	0.004	0.03	0.04	0.12
3 (Hg2-C15)	0.007	0.06	0.07	N/A
4 (Hg3-O2)	0.001	1.362	0.12	1.34
5 (Hg1'-O1)	0.003	0.07	0.08	0.24
6 (Hg1'-O2)	0.003	0.07	0.09	0.24
7 (Hg2'-C6)	0.006	0.04	0.06	0.31
8 (Hg3'-C2)	0.006	0.03	0.05	0.32

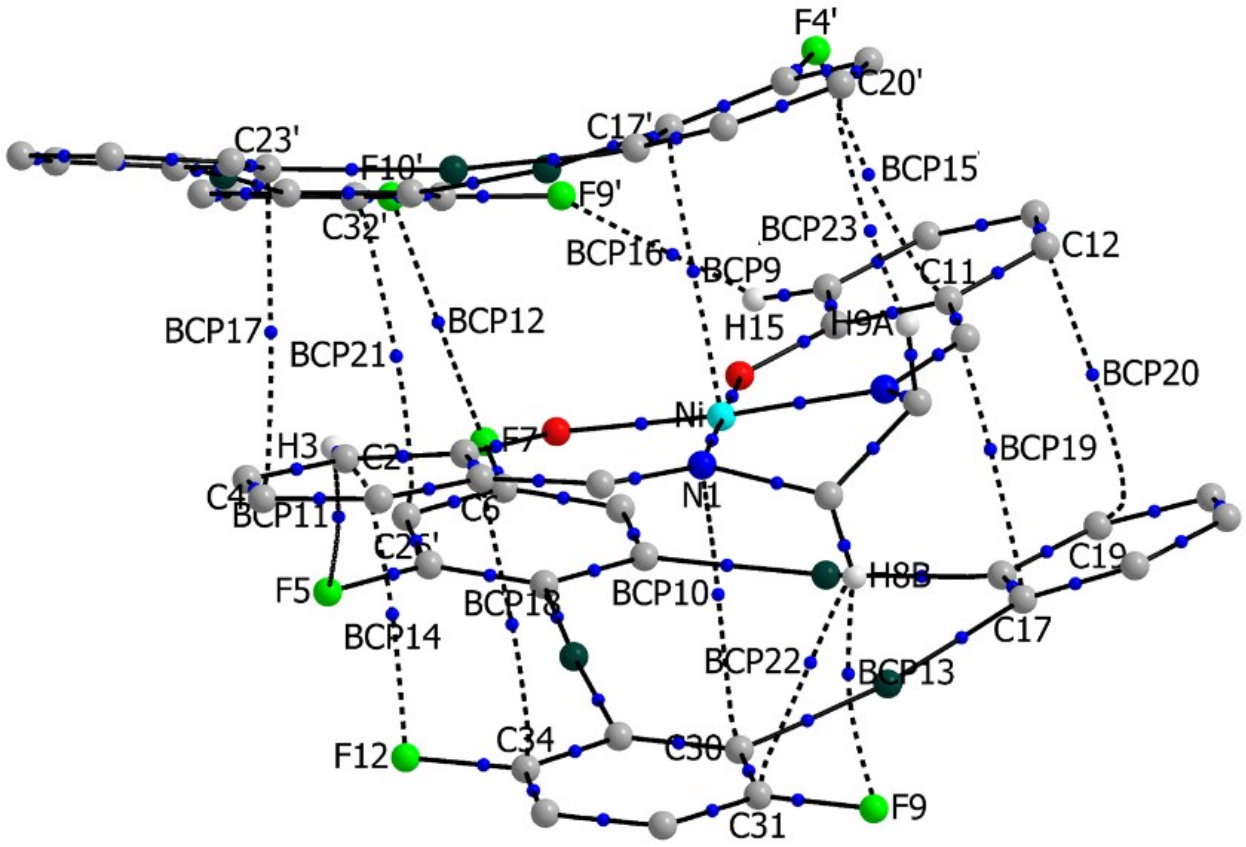

Figure S5. xyz plot of [**B**-(Ni(salen))], showing labeled BCPs cooresponding to intermolecular contacts not involving mercury. BCPs are represented by blue spheres. Selected fluorine and hydrogen atoms are omitted for clarity.

Table S9. Selected features of the electron density distribution function at BCPs cooresponding to intermolecular contacts not involving mercury in [**B**-(Ni(salen))].

BCP No. (A-B)	$d_{A\text{-}BCP}$ (Å)	$d_{B\text{-}BCP}$ (Å)	ρ_{BCP} (e Å^{-3})	$\nabla^2\rho_{BCP}$ (e Å^{-5})	ε
9 (Ni-C17')	1.584	1.608	0.06	0.67	0.59
10 (N1-C30)	1.766	1.766	0.04	0.37	4.24
11 (F5-H2)	1.717	1.355	0.01	0.22	0.25
12 (F7-F10)	1.544	1.537	0.02	0.61	0.29
13 (F9-H8B)	1.494	1.062	0.05	0.81	3.05
14 (F12-C2)	1.573	1.786	0.03	0.45	1.80
15 (F4'-C11)	1.468	1.626	0.05	0.74	0.84
16 (F9'-H15)	1.410	1.031	0.05	0.91	0.12
17 (C4-C23')	1.794	1.817	0.03	0.29	2.39
18 (C6-C34)	1.670	1.722	0.05	0.39	0.56
19 (C11-C17)	1.691	1.683	0.05	0.47	2.95
20 (C12-C19)	1.841	1.781	0.04	0.36	2.78

21 (C26-C32')	1.785	1.798	0.02	0.26	0.30
22 (C31-H8B)	1.575	1.090	0.05	0.72	1.06
23 (C20'-H9A)	1.631	1.113	0.04	0.57	0.38

Table S10. Selected derivative features of the electron density distribution function at BCPs cooresponding to intermolecular contacts not involving mercury in [**B**-(Ni(salen))].

BCP No. (A-B)	H_{BCP} (Hartree Å^{-3})	G_{BCP} (Hartree Å^{-3})	δ(A,B)	$\oint_{A\cap B}\rho(r)$ (e Å^{-1}) [a]
9 (Ni-C17')	0.007	0.04	0.04	N/A
10 (N1-C30)	0.003	0.02	0.02	0.08
11 (F5-H2)	0.005	0.01	0.01	0.02
12 (F7-F10)	0.009	0.03	0.01	0.04
13 (F9-H8B)	0.011	0.05	0.02	0.06
14 (F12-C2)	0.007	0.02	0.01	0.07
15 (F4'-C11)	0.009	0.04	0.02	N/A
16 (F9'-H15)	0.011	0.05	0.02	0.10
17 (C4-C23')	0.003	0.02	0.01	0.13
18 (C6-C34)	0.005	0.02	0.02	0.10
19 (C11-C17)	0.005	0.03	0.02	N/A
20 (C12-C19)	0.005	0.02	0.01	N/A
21 (C26-C32')	0.003	0.01	0.01	N/A
22 (C31-H8B)	0.011	0.04	0.01	N/A
23 (C20'-H9A)	0.009	0.03	0.02	0.07

a) Some values of $\oint_{A\cap B}\rho(r)$ (e Å^{-1}) could not be determined, due to integration of some atoms with the 'Promega' algorithm instead of the 'Proaim' algorithm within the AIMAll program.

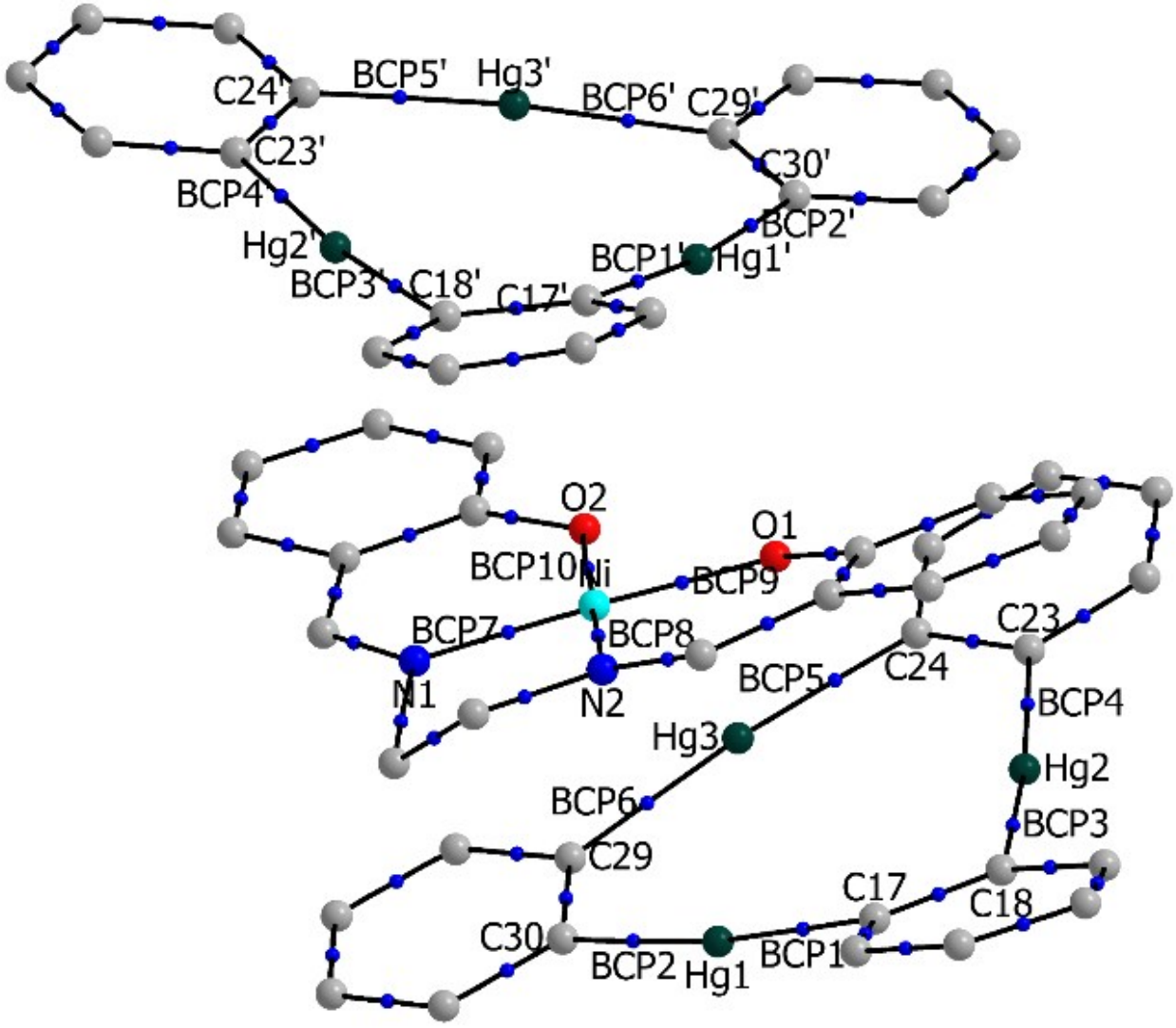

Figure S6. xyz plot of [**B**-(Ni(salen))], showing labeled BCPs cooresponding to selected intramolecular bonds in **B** and Ni(salen). BCPs are represented by blue spheres. Fluorine and hydrogen atoms are omitted for clarity.

Table S11. Selected features of the electron density distribution function at selected intramolecular BCPs in [**B**-(Ni(salen))].

BCP No. (A-B)	$d_{A\text{-}BCP}$ (Å)	$d_{B\text{-}BCP}$ (Å)	ρ_{BCP} (e Å^{-3})	$\nabla^2\rho_{BCP}$ (e Å^{-5})	ε
1 (Hg1-C17)	1.135	0.948	0.88	2.78	0.04
1' (Hg1'-C17')	1.130	0.952	0.88	3.13	0.03
2 (Hg1-C30)	1.135	0.949	0.87	2.83	0.04
2' (Hg1'-C30')	1.134	0.950	0.87	2.89	0.04
3 (Hg2-C18)	1.128	0.944	0.89	3.08	0.04
3' (Hg2'-C18')	1.133	0.943	0.89	2.99	0.04
4 (Hg2-C23)	1.133	0.946	0.88	2.80	0.04
4' (Hg2'-C23')	1.129	0.946	0.88	2.79	0.04
5 (Hg3-C24)	1.132	0.945	0.89	2.84	0.03
5' (Hg3'-C24')	1.131	0.946	0.88	2.90	0.04
6 (Hg3-C29)	1.130	0.952	0.88	3.16	0.03
6' (Hg3'-C29')	1.134	0.948	0.88	2.79	0.04
7 (Ni-N1)	0.889	0.964	0.85	13.70	0.04
8 (Ni-N2)	0.891	0.965	0.84	13.7	0.03
9 (Ni-O1)	0.893	0.957	0.73	15.85	0.09
10 (Ni-O2)	0.895	0.959	0.71	15.72	0.10

Table S12. Selected derivative features of the electron density distribution function at selected intramolecular BCPs in [**B**-(Ni(salen))].

BCP No. (A-B)	H_{BCP} (Hartree Å^{-3})	G_{BCP} (Hartree Å^{-3})	δ(A,B)	$\oint_{A\cap B}\rho(r)$ (e Å^{-1}) [a]
1 (Hg1-C17)	-0.41	0.61	0.88	1.83
1' (Hg1'-C17')	-0.41	0.63	0.85	1.83
2 (Hg1-C30)	-0.41	0.61	0.87	1.89
2' (Hg1'-C30')	-0.41	0.61	0.87	1.81
3 (Hg2-C18)	-0.42	0.64	0.87	1.88
3' (Hg2'-C18')	-0.43	0.63	0.87	1.85
4 (Hg2-C23)	-0.42	0.61	0.87	N/A
4' (Hg2'-C23')	-0.42	0.61	0.88	1.85
5 (Hg3-C24)	-0.42	0.62	0.88	1.83
5' (Hg3'-C24')	-0.42	0.62	0.88	1.90
6 (Hg3-C29)	-0.41	0.63	0.85	1.84
6' (Hg3'-C29')	-0.41	0.61	0.88	1.86
7 (Ni-N1)	-0.22	1.18	0.71	1.56
8 (Ni-N2)	-0.22	1.17	0.70	N/A
9 (Ni-O1)	-0.06	1.17	0.61	N/A
10 (Ni-O2)	-0.06	1.17	0.61	N/A

a) Some values of $\oint_{A\cap B}\rho(r)$ (e Å^{-1}) could not be determined, due to integration of some atoms with the 'Promega' algorithm instead of the 'Proaim' algorithm within the AIMAll program.

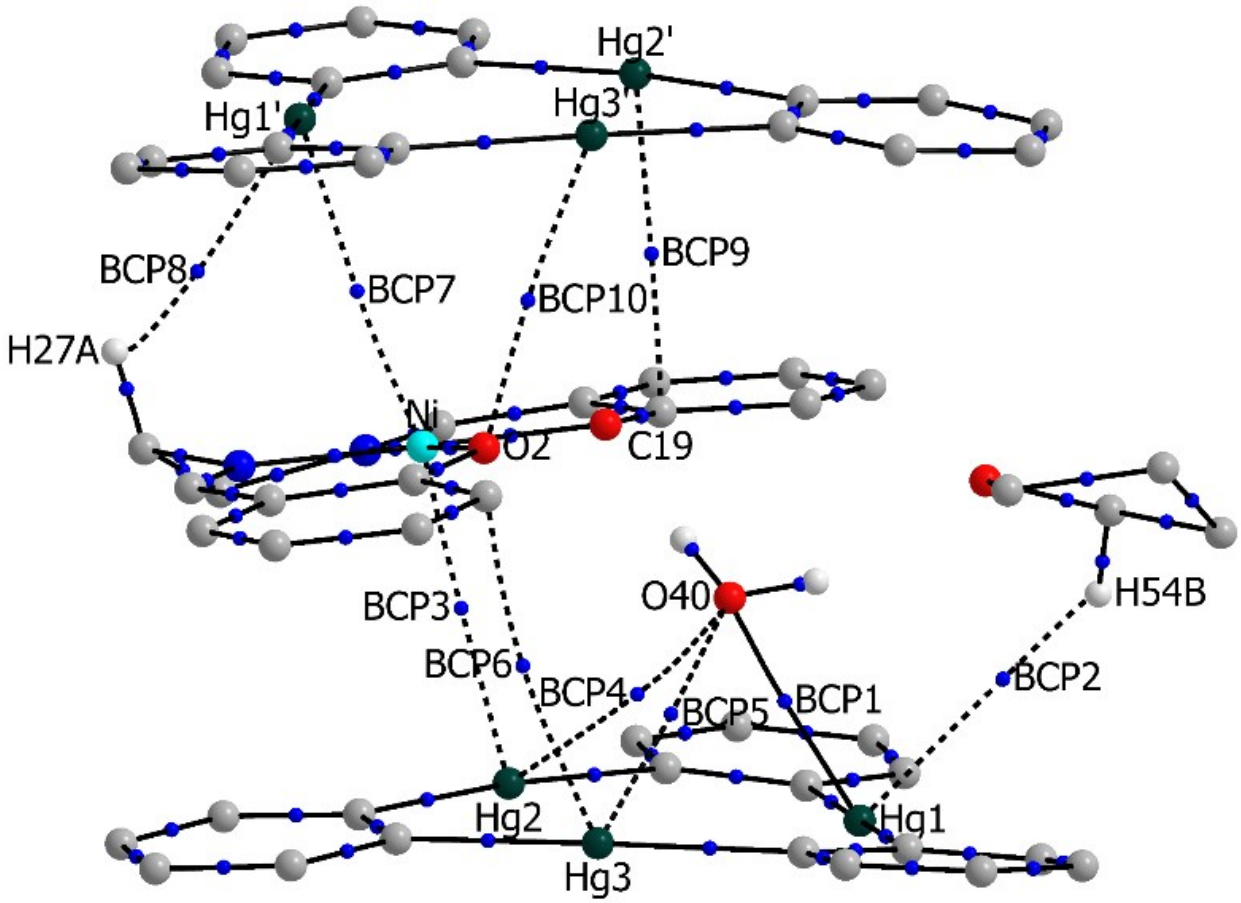

Figure S7. xyz plot of [**B**-(Ni(salen))-THF-H_2O], showing labeled BCPs cooresponding to intermolecular interactions involving mercury. BCPs are represented by blue spheres. Fluorine and selected hydrogen atoms are omitted for clarity.

Table S13. Selected features of the electron density distribution function at BCPs cooresponding to intermolecular interactions involving mercury in [**B**-(Ni(salen))-THF-H_2O].

BCP No. (A-B)	$d_{A\text{-}BCP}$ (Å)	$d_{B\text{-}BCP}$ (Å)	ρ_{BCP} (e Å^{-3})	$\nabla^2\rho_{BCP}$ (e Å^{-5})	ε
1 (Hg1-O40)	1.452	1.235	0.19	2.48	0.07
2 (Hg1-H54B)	1.978	1.245	0.03	0.33	0.10
3 (Hg2-Ni)	1.765	1.617	0.07	0.64	0.07
4 (Hg2-O40)	1.811	1.595	0.05	0.57	0.15
5 (Hg3-O40)	1.662	1.453	0.08	1.00	0.05
6 (Hg3-C33)	1.908	1.718	0.04	0.37	0.24
7 (Hg1'-Ni)	1.768	1.639	0.07	0.66	0.28
8 (Hg1'-H27A)	1.856	1.177	0.04	0.56	0.69
9 (Hg2'-C19)	1.776	1.541	0.06	0.68	0.42

10 (Hg3'-O2)	1.743	1.520	0.06	0.72	0.26

Table S14. Selected derivative features of the electron density distribution function at BCPs cooresponding to intermolecular interactions involving mercury in [**B**-(Ni(salen))-THF-H_2O].

BCP No. (A-B)	H_{BCP} (Hartree Å^{-3})	G_{BCP} (Hartree Å^{-3})	δ(A,B)	$\oint_{A\cap B}\rho(r)$ (e Å^{-1}) [a]
1 (Hg1-O40)	0.001	0.17	0.21	0.55
2 (Hg1-H54B)	0.005	0.02	0.02	0.07
3 (Hg2-Ni)	0.005	0.04	0.08	0.31
4 (Hg2-O40)	0.005	0.04	0.05	0.10
5 (Hg3-O40)	0.005	0.06	0.08	0.21
6 (Hg3-C33)	0.005	0.02	0.03	0.15
7 (Hg1'-Ni)	0.005	0.04	0.08	0.41
8 (Hg1'-H27A)	0.009	0.03	0.02	0.09
9 (Hg2'-C19)	0.008	0.04	0.04	N/A
10 (Hg3'-O2)	0.004	0.05	0.06	0.24

a) Some values of $\oint_{A\cap B}\rho(r)$ (e Å^{-1}) could not be determined, due to integration of some atoms with the 'Promega' algorithm instead of the 'Proaim' algorithm within the AIMAll program.

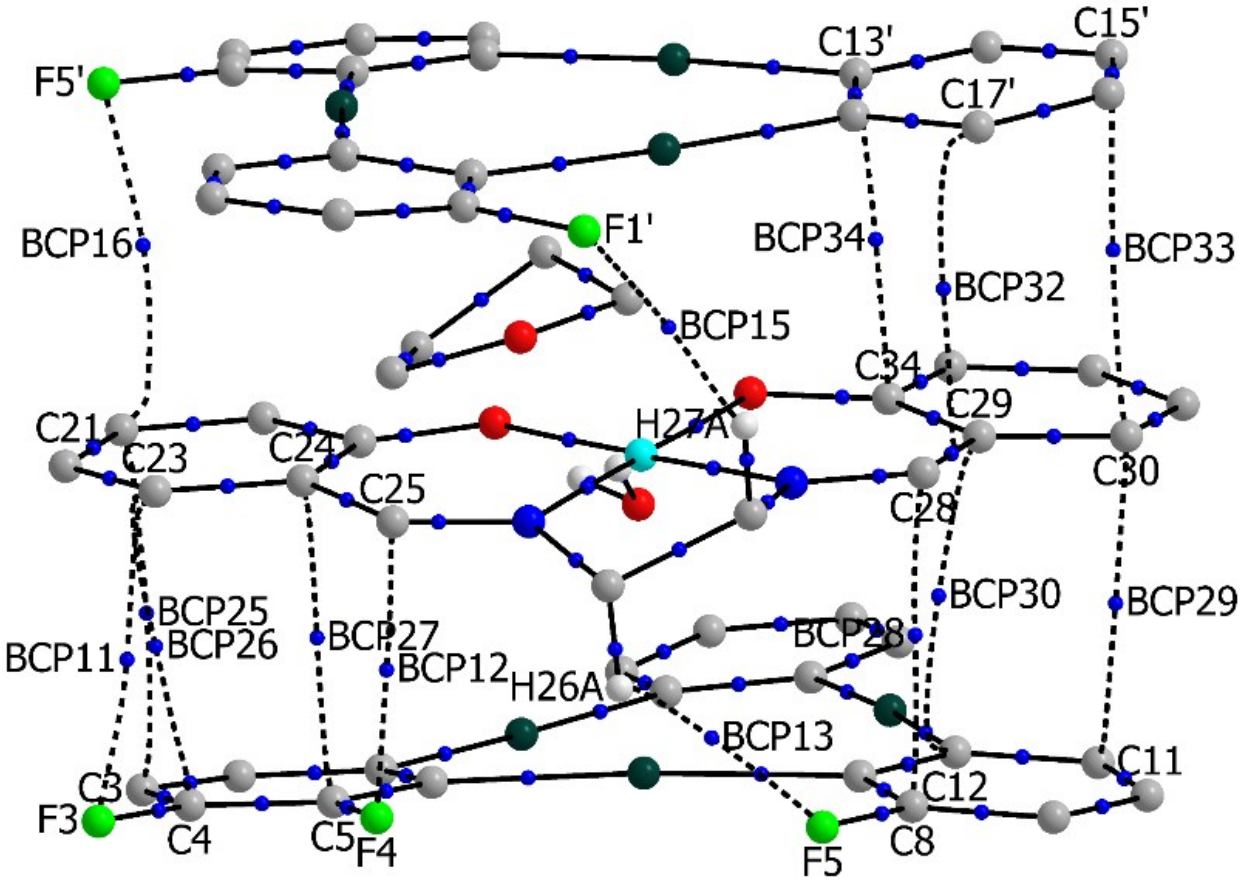

Figure S8. xyz plot of [**B**-(Ni(salen))-THF-H_2O], showing labeled BCPs cooresponding to intermolecular contacts not involving mercury between **B** and Ni(salen). BCPs are represented by blue spheres. Selected fluorine and hydrogen atoms are omitted for clarity.

Table S15. Selected features of the electron density distribution function at BCPs cooresponding to intermolecular contacts not involving mercury between **B** and Ni(salen) in [**B**-(Ni(salen))-THF-H_2O].

BCP No. (A-B)	$d_{A\text{-}BCP}$ (Å)	$d_{B\text{-}BCP}$ (Å)	ρ_{BCP} (e Å^{-3})	$\nabla^2\rho_{BCP}$ (e Å^{-5})	ε
11 (F3-C23)	1.557	1.746	0.03	0.50	0.93
12 (F4-C25)	1.481	1.541	0.05	0.72	0.57
13 (F5-H26A)	1.504	1.151	0.03	0.62	0.18
15 (F1'-H27A)	1.693	1.299	0.02	0.29	8.91
16 (F5'-C21)	1.591	1.773	0.03	0.42	2.59
25 (C3-C21)	1.757	1.765	0.03	0.33	1.57
26 (C4-C23)	1.666	1.811	0.03	0.41	1.00
27 (C5-C24)	1.635	1.713	0.04	0.44	0.77
28 (C8-C28)	1.654	1.621	0.04	0.48	0.28
29 (C11-C30)	1.694	1.701	0.04	0.42	0.93

30 (C12-C29)	1.801	1.762	0.04	0.38	1.48
32 (C29-C17')	1.768	1.805	0.04	0.41	0.53
33 (C30-C15')	1.849	1.801	0.03	0.30	7.90
34 (C34-C13')	1.649	1.582	0.05	0.56	0.89

Table S16. Selected derivative features of the electron density distribution function at BCPs cooresponding to intermolecular contacts not involving mercury between **B** and Ni(salen) in [**B**-(Ni(salen))-THF-H_2O].

BCP No. (A-B)	H_{BCP} (Hartree Å^{-3})	G_{BCP} (Hartree Å^{-3})	δ(A,B)	$\oint_{A\cap B}\rho(r)$ (e Å^{-1}) [a]
11 (F3-C23)	0.007	0.03	0.02	0.06
12 (F4-C25)	0.09	0.04	0.02	0.13
13 (F5-H26A)	0.011	0.03	0.02	0.06
15 (F1'-H27A)	0.006	0.01	0.01	0.02
16 (F5'-C21)	0.007	0.02	0.01	0.05
25 (C3-C21)	0.004	0.02	0.01	0.13
26 (C4-C23)	0.005	0.02	0.01	0.06
27 (C5-C24)	0.005	0.03	0.02	0.18
28 (C8-C28)	0.007	0.03	0.02	0.21
29 (C11-C30)	0.005	0.02	0.02	0.21
30 (C12-C29)	0.004	0.02	0.01	0.12
32 (C29-C17')	0.005	0.02	0.01	N/A
33 (C30-C15')	0.004	0.02	0.01	N/A
34 (C34-C13')	0.008	0.03	0.02	N/A

a) Some values of $\oint_{A\cap B}\rho(r)$ (e Å^{-1}) could not be determined, due to integration of some atoms with the 'Promega' algorithm instead of the 'Proaim' algorithm within the AIMAll program.

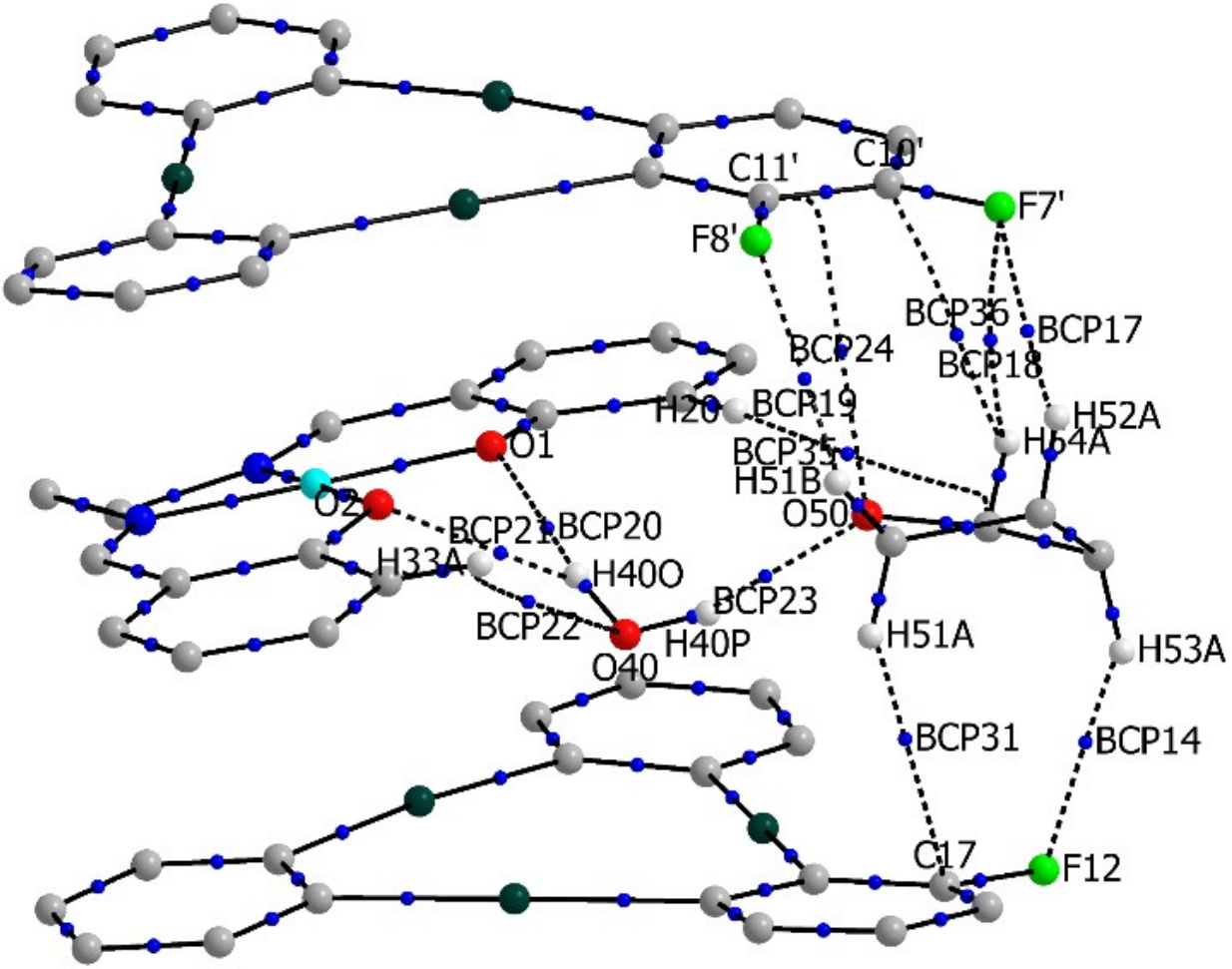

Figure S9. xyz plot of [**B**-(Ni(salen))-THF-H_2O], showing labeled BCPs cooresponding to intermolecular contacts involving the H_2O and THF molecules. BCPs are represented by blue spheres. Selected fluorine and hydrogen atoms are omitted for clarity.

Table S17. Selected features of the electron density distribution function at BCPs cooresponding to intermolecular contacts involving the H_2O and THF molecules in [**B**-(Ni(salen))-THF-H_2O].

BCP No. (A-B)	$d_{A\text{-}BCP}$ (Å)	$d_{B\text{-}BCP}$ (Å)	ρ_{BCP} (e Å^{-3})	$\nabla^2\rho_{BCP}$ (e Å^{-5})	ε
14 (F12-H53A)	1.441	1.051	0.05	0.87	0.01
17 (F7'-H52A)	1.486	1.141	0.04	0.66	0.12
18 (F7'-H54)	1.580	1.241	0.03	0.51	1.17
19 (F8'-H51B)	1.490	1.129	0.04	0.68	0.09
20 (O1-H40O)	1.385	0.846	0.09	1.30	0.07
21 (O2-H40O)	1.336	0.834	0.11	1.65	0.14
22 (O40-H33A)	1.661	1.228	0.03	0.50	0.41
23 (O50-H40P)	1.289	0.758	0.15	1.90	0.06
24 (O50-C11')	1.730	1.670	0.04	0.45	1.80

31 (C17-H51A)	1.741	1.193	0.04	0.45	2.29
35 (C54-H20)	2.158	1.594	0.01	0.06	0.54
36 (C10'-H54A)	1.706	1.256	0.03	0.41	4.09

Table S18. Selected derivative features of the electron density distribution function at BCPs cooresponding to intermolecular contacts involving the H_2O and THF molecules in [**B**-(Ni(salen))-THF-H_2O].

BCP No. (A-B)	H_{BCP} (Hartree Å^{-3})	G_{BCP} (Hartree Å^{-3})	δ(A,B)	$\oint_{A\cap B}\rho(r)$ (e Å^{-1}) [a]
14 (F12-H53A)	0.01	0.05	0.02	0.16
17 (F7'-H52A)	0.01	0.04	0.02	0.07
18 (F7'-H54)	0.009	0.03	0.01	0.04
19 (F8'-H51B)	0.011	0.04	0.02	0.07
20 (O1-H40O)	0.005	0.09	0.03	N/A
21 (O2-H40O)	0.006	0.11	0.02	N/A
22 (O40-H33A)	0.008	0.03	0.02	0.06
23 (O50-H40P)	-0.004	0.14	0.05	N/A
24 (O50-C11')	0.006	0.03	0.02	N/A
31 (C17-H51A)	0.007	0.02	0.01	0.18
35 (C54-H20)	0.001	0.003	0.002	0.01
36 (C10'-H54A)	0.007	0.02	0.01	N/A

a) Some values of $\oint_{A\cap B}\rho(r)$ (e Å^{-1}) could not be determined, due to integration of some atoms with the 'Promega' algorithm instead of the 'Proaim' algorithm within the AIMAll program.

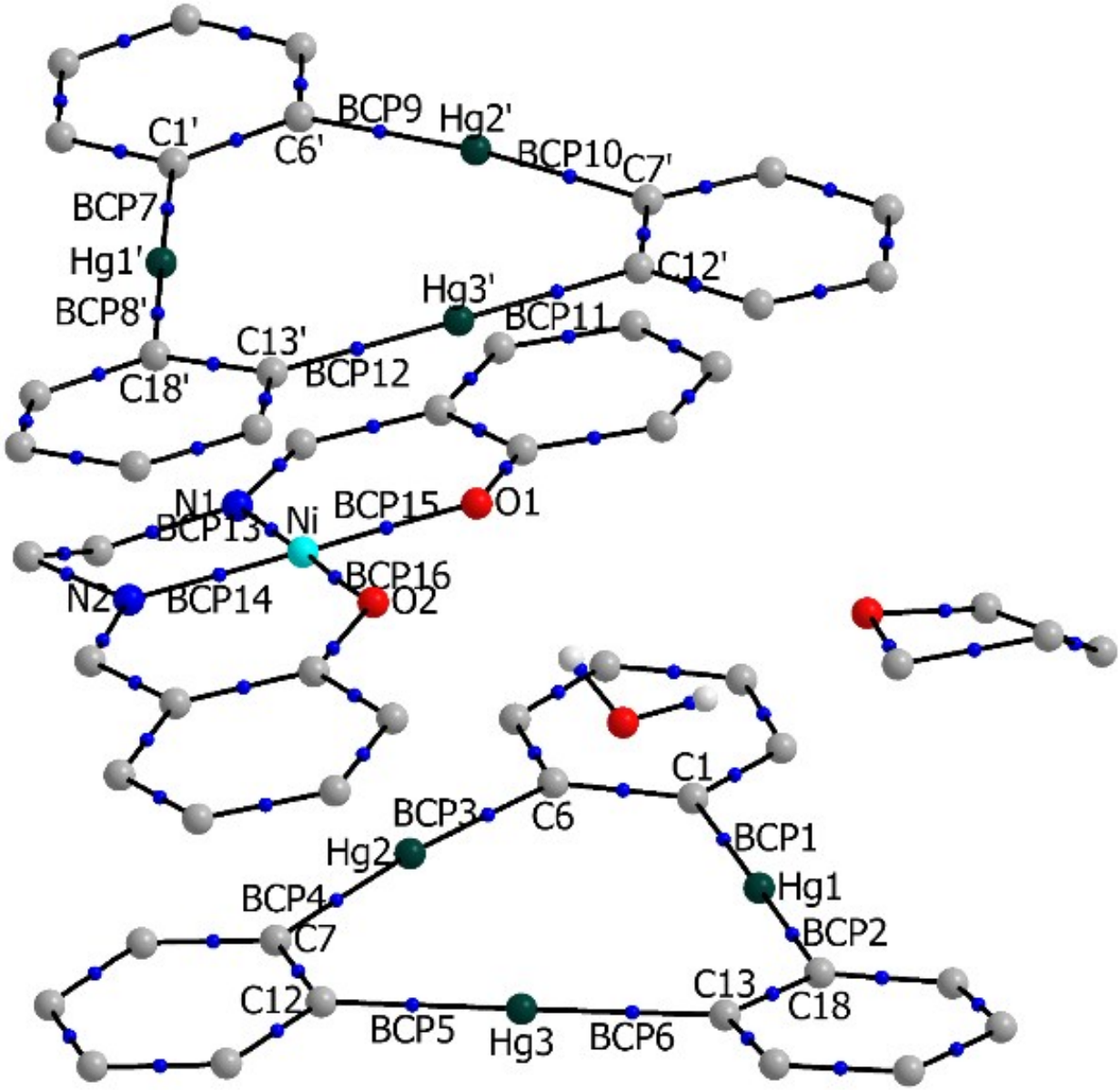

Figure S10. xyz plot of [**B**-(Ni(salen))-THF-H_2O], showing labeled BCPs cooresponding to selected intramolecular bonds in **B** and Ni(salen). BCPs are represented by blue spheres. Fluorine and selected hydrogen atoms are omitted for clarity.

Table S19. Selected features of the electron density distribution function at selected intramolecular BCPs in [**B**-(Ni(salen))-THF-H_2O].

BCP No. (A-B)	$d_{A\text{-}BCP}$ (Å)	$d_{B\text{-}BCP}$ (Å)	ρ_{BCP} (e Å^{-3})	$\nabla^2\rho_{BCP}$ (e Å^{-5})	ε
1 (Hg1-C1)	1.129	0.946	0.89	3.04	0.04
2 (Hg1-C18)	1.129	0.946	0.89	3.02	0.04
3 (Hg2-C6)	1.125	0.937	0.90	2.96	0.04
4 (Hg2-C7)	1.129	0.945	0.89	2.97	0.04

5 (Hg3-C12)	1.124	0.941	0.91	3.12	0.04
6 (Hg3-C13)	1.123	0.938	0.91	3.04	0.04
7 (Hg1'-C1')	1.130	0.945	0.89	2.93	0.04
8 (Hg1'-C18')	1.132	0.943	0.89	2.74	0.04
9 (Hg2'-C6')	1.124	0.938	0.91	3.08	0.04
10 (Hg2'-C7')	1.130	0.943	0.89	2.80	0.04
11 (Hg3'-C12')	1.123	0.939	0.91	2.95	0.04
12 (Hg3'-C13')	1.125	0.938	0.91	3.04	0.04
13 (Ni-N1)	0.883	0.953	0.88	14.18	0.03
14 (Ni-N2)	0.886	0.959	0.86	13.85	0.03
15 (Ni-O1)	0.888	0.948	0.75	16.47	0.08
16 (Ni-O2)	0.890	0.951	0.74	16.15	0.08

Table S20. Selected derivative features of the electron density distribution function at selected intramolecular BCPs in [**B**-(Ni(salen))-THF-H_2O].

BCP No. (A-B)	H_{BCP} (Hartree Å^{-3})	G_{BCP} (Hartree Å^{-3})	δ(A,B)	$\oint_{A\cap B}\rho(r)$ (e Å^{-1}) [a]
1 (Hg1-C1)	-0.42	0.63	0.87	1.85
2 (Hg1-C18)	-0.42	0.63	0.86	1.86
3 (Hg2-C6)	-0.44	0.65	0.88	1.88
4 (Hg2-C7)	-0.43	0.63	0.87	1.85
5 (Hg3-C12)	-0.44	0.66	0.88	1.87
6 (Hg3-C13)	-0.44	0.65	0.88	1.85
7 (Hg1'-C1')	-0.42	0.63	0.87	1.94
8 (Hg1'-C18')	-0.43	0.62	0.87	1.88
9 (Hg2'-C6')	-0.44	0.66	0.88	N/A
10 (Hg2'-C7')	-0.43	0.62	0.88	N/A
11 (Hg3'-C12')	-0.44	0.65	0.88	1.86
12 (Hg3'-C13')	-0.44	0.66	0.88	1.91
13 (Ni-N1)	-0.25	1.24	0.72	1.67
14 (Ni-N2)	-0.23	1.20	0.71	1.63
15 (Ni-O1)	-0.08	1.23	0.63	N/A
16 (Ni-O2)	-0.07	1.20	0.62	N/A

a) Some values of $\oint_{A\cap B}\rho(r)$ (e Å^{-1}) could not be determined, due to integration of some atoms with the 'Promega' algorithm instead of the 'Proaim' algorithm within the AIMAll program.